Interannual drought length governs dissolved organic carbon dynamics in blackwater rivers of the western upper Suwannee River basin

A. S. Mehring,[1,2] R. R. Lowrance,[3] A. M. Helton,[4] C. M. Pringle,[1] A. Thompson,[5] D. D. Bosch,[3] and G. Vellidis[5]

[1] The Little River (LR) in southern Georgia, U.S., has experienced lengthening droughts since monitoring began in 1972. We evaluated the impacts of drought on riverine carbon cycling using a 9 year data set of dissolved organic carbon (DOC) coupled with laboratory experiments in the LR, as well as long-term data sets in three additional rivers within the Suwannee River basin. Longer drought periods reduced downstream DOC export but also led to higher DOC concentrations in the following hydroperiod. Within a hydroperiod, DOC concentration was positively correlated with temperature and negatively correlated with river discharge but also negatively correlated with total discharge during the previous hydroperiod. Among hydroperiods, DOC concentration was more strongly correlated with antecedent hydrological conditions than with current hydrological conditions across broad spatial scales: in three additional rivers within the Suwannee River basin (Alapaha, Withlacoochee, and Okapilco) and in headwater and downstream reaches of the LR. Microbial DOC consumption and CO_2 production were elevated when DOC concentration was high. Despite dramatic hydrologic changes, DOC composition appeared stable, with optical analyses suggesting that LR DOC is primarily composed of three terrestrial humic-like fluorescence groups. If the current climatic trend of intensifying droughts, elevated temperatures and decreased discharge continue, our results suggest the net effect may be for a more localized riverine carbon cycle with reduced downstream transport of DOC, but higher local mineralization rates due to elevated DOC concentrations.

1. Introduction

[2] In many world regions, rainfall and river discharge have been decreasing or are predicted to decrease over time [*Dai et al.*, 2009; *Solomon et al.*, 2009], with the potential to decrease riverine solute flux [*Lutz et al.*, 2012] including dissolved organic carbon (DOC). Within rivers, DOC strongly influences microbial production, respiration, and ecosystem metabolism [*Findlay et al.*, 2003; *Hanson et al.*, 2003; *Wiegner et al.*, 2005]. While almost half of the carbon inputs to rivers are released to the atmosphere as carbon dioxide (CO_2) and methane (CH_4) before reaching estuaries [*Cole et al.*, 2007], rivers provide the largest contribution of terrestrially derived DOC (0.3 Pg C y^{-1}) to ocean carbon budgets [*Meybeck*, 1982]. As such, drought-related disruptions of DOC flux may impact secondary production in rivers and lakes [*Berggren et al.*, 2010], gradients of marine phytoplankton biomass around river plumes [*Bledsoe and Phlips*, 2000], and potential priming effects of terrigenous DOC on marine carbon cycling [*Bianchi*, 2011].

[3] However, DOC flux is influenced both by river discharge and DOC concentration, and while reduced river discharge may result in a lower volume of water available for transport, local atmospheric conditions and in-stream processes may elevate DOC concentration ([DOC]). Rising [DOC] in many aquatic ecosystems around the world has been explained by an array of causative factors, including decreased ionic strength [*Monteith et al.*, 2007], physical disturbance of the terrestrial landscape [*Rixen et al.*, 2008],

Figure 1. The Suwannee River basin. Letters indicate locations of sampling stations in the Alapaha (AR), Little (LR), Okapilco (OC), and Withlacoochee (WR) Rivers. The focal site (LR2) is indicated with a white circle. The inset shows the Suwannee River basin's location in the southeastern United States.

continuing nitrogen deposition [*Findlay*, 2005], rising CO_2 and temperature [*Freeman et al.*, 2001; *Freeman et al.*, 2004], decreased river discharge [*Eimers et al.*, 2008], and intensifying droughts [*Pärn and Mander*, 2012]. While rising [DOC] may mitigate the negative effects of reduced discharge on DOC flux, carbon mineralization rates are often positively correlated to [DOC] [*Chow et al.*, 2006; *Lundquist et al.*, 1999] and to temperature [*Kankaala and Bergström*, 2004; *Pulliam*, 1993]. Therefore, it is possible further increases in [DOC] [*Larsen et al.*, 2011] will increase mineralization and thus exacerbate, rather than counteract, reduced DOC flux during periods of reduced river discharge.

[4] The southeastern U.S. has experienced significant decreases in warm season precipitation and increases in cold season precipitation during the past century [*Alexandrov and Hoogenboom*, 2001; *Stahle and Cleaveland*, 1992]. However, prior to the 1900s the region may have received lower rainfall and experienced droughts of greater severity than those in more recent years [*Pederson et al.*, 2012; *Seager et al.*, 2009]. Droughts of equal or greater intensity than those in the past century are predicted to occur in the southeastern U.S. in the future [*Dai*, 2010]. This will likely impact the many rivers in this region, so-called blackwater rivers, which export a large amount of DOC relative to their discharge [*Mulholland and Kuenzler*, 1979; *Schlesinger and Melack*, 1981] and are globally important suppliers of DOC to the world's oceans [*Baum et al.*, 2007; *Beck et al.*, 1974; *Raymond and Bauer*, 2001]. Determining how DOC export is affected by low flow events in blackwater rivers is critical to predicting drought-induced changes in riverine carbon cycling globally.

[5] In this study, we evaluate the impact of reduced rainfall and discharge on DOC cycling in four blackwater rivers within the Suwannee River basin in south central Georgia, U.S., to determine the environmental drivers and temporal patterns of DOC characteristics and export. A 9 year data set of weekly DOC samples encompassing a large gradient in rainfall and discharge was complimented with contemporary (2008–2009) optical analysis of DOC and laboratory incubations to characterize changes in composition, bioavailability, and potential mineralization rates.

2. Methods

2.1. Site Description

[6] The focal site (Figure 1, LR2) is a fifth-order watershed in the Little River (LR), a blackwater river in Tift County, Georgia, U.S., draining the Atlantic coastal plain of North America. The study reach (31°28′54″, 83°35′03″) drains the entire 33,400 ha Little River Experimental Watershed (LREW) [*Bosch et al.*, 2007]. Discharge is highly variable; like many other headwaters within the Tifton Upland of Georgia's coastal plain, the upper reaches of the LR typically dry completely during summer and fall [*Meyer*, 1992]. The Hawthorne formation, an aquiclude consisting of clay stone and sandstone, separates surface water from the underlying aquifer, uncoupling river discharge from the Floridan aquifer system [*Sheridan*, 1997]. A summary of physical and chemical data is provided in Table S1 in the supporting information.

[7] Effects in the focal site (LR2) were compared to two other sites in the Little River, as well as three sites in other watersheds of the Suwannee River Basin (Figure 1). LR1 is an intermittent third-order reach (31°41′32″, 83°42′09″) meandering through a second-growth forested floodplain, draining a 2210 ha catchment within the LREW. LR1 and LR2 are gauged with broad-crested V notch weirs operated by the United States Department of Agriculture-Agricultural Research Service [*Bosch and Sheridan*, 2007; *Bosch et al.*, 2007]. LR3 is an open channel flow site installed in conjunction with U.S. Geological Survey (USGS) site 02318000 (31°09′36″, 83°32′36″) on the Little River at the dam outlet of Reed Bingham Lake. The drainage area of the watershed is 149,440 ha. The Alapaha River (AR), Withlacoochee River (WR), and Okapilco Creek (OC) sites (Figure 1) are also open channel flow sites, installed in conjunction with USGS sites 02316000, 023177483, and 02318700, respectively. AR (31°23′04″, 83°11′33″) drains a 171,720 ha watershed, WR (30°56′56″, 83°16′19″) drains a 130,020 ha watershed, and OC (30°49′33″, 83°33′45″) drains a 69,670 ha watershed.

2.2. Field Methods

[8] Streamflow and rainfall data collection methods for site LR2 are described by *Bosch and Sheridan* [2007] and by *Bosch et al.* [2007]. Dissolved oxygen (DO) and temperature were recorded at 15 min intervals from October 2002 (beginning of a hydroperiod) to June 2009, using submersible DO (Sensorex DO6000) and temperature sensors (Campbell Scientific, CS107). DO and temperature were also measured weekly using a hand-held Yellow Springs Instruments (YSI) 6600 V2 Sonde. Automated and hand-held measurements were averaged when both were available.

[9] Flow proportional composite water samples in LR1 and LR2 were collected from October 2002 to May 2010 using an automated Teledyne Isco, Inc. model 3710 sampler, immediately deposited in a refrigerated (4°C) housing [*Feyereisen et al.*, 2007], and returned to the laboratory for chemical analysis. The same methods were used in sites AR and LR3 from January 2004 to January 2010 and in sites OC

and WR from January 2006 to May 2010. Additional weekly grab samples were collected for analysis of chlorophyll *a* (chl *a*) in LR2 from January 2003 to May 2006. From 1981–1988, discrete (grab) water samples were also collected from site LR2. Water depth upstream of station LR2 was measured monthly from January 2007 to December 2008. Depth was sampled at 49 points spaced 25 m apart along five parallel transects running across the wetted channel. Transects were spaced ~150 m apart longitudinally. As discharge was continuously measured at the weir at LR2, we fit a power equation to extrapolate average water depth based on river discharge on any date (equation (1)) [*Leopold and Maddock*, 1953]:

$$H = 2.49 \times Q^{0.39} \tag{1}$$

where H = average water depth (cm) in the channel upstream from the weir and Q = discharge (L s^{-1}). Liters of water per 1 m^2 (V_a, in L m^{-2}) was calculated as

$$V_a = H \times \frac{1000 \ L}{m^3} \tag{2}$$

where H = average water depth (m) in the river (equation (1)).

2.3. Chemical Analysis

[10] In the laboratory, water samples were filtered through glass fiber filters (Whatman, 934-AH, nominal pore size 1 μm) and immediately frozen (−20°C). DOC was analyzed with a Shimadzu 5050A total organic carbon analyzer (method 5310B) [*American Public Health Association (APHA)*, 1999] for samples collected from 2002 to 2010 and with a Technicon Autoanalyzer II (Technicon method No. 451-76 W) [*APHA*, 1999] for samples collected from 1981 to 1988. Dissolved NO$_3^-$ + NO$_2^-$ − N, NH$_4^+$ − N, Cl$^-$, and PO$_4^{3-}$ − P were analyzed using Environmental Protection Agency (EPA)-approved colorimetric techniques [*APHA*, 1999]. Total Kjeldahl N and total P were determined on digests of unfiltered samples using Lachat flow injection analyzers (Lachat Instruments, 1997). Chl *a* was determined based on United States Environmental Protection Agency method 445.0 [*United States Environmental Protection Agency*, 1998] and standard method 10200H [*APHA*, 1999] using a Turner Designs TD700 fluorometer. Water samples collected from January 2008 to June 2010 were analyzed for Fe concentration with inductively coupled plasma mass spectroscopy (Perkin Elmer Elan 6000).

2.4. DOC Bioavailability Assays

[11] For site LR2, 7 day, dark, oxic laboratory DOC bioavailability assays were conducted using methods described in *McDowell et al.* [2006]. Water samples (20 mL) were filtered into acid-washed, autoclaved 160 mL serum bottles (hereafter "chambers") through sterile 0.2 μm polyethersulfone membrane filters (Whatman Puradisc$^{™}$) mounted on glass syringes. Filtered water of 5 mL was immediately acidified and analyzed for [DOC]. Microbial inoculum (150 μL unfiltered river water collected on 8 June 2009) was added, with 30 μL of nutrient solution (0.1% NH$_4$NO$_3$ + 0.1% K$_2$HPO$_4$) to prevent nutrient limitation. Blanks were run as deionized water with added nutrients and inoculum. Chambers were immediately sealed with gas tight septa caps, kept in the dark at 20°C for 7 days, and agitated every 24 h.

[12] After 7 days, 1 cc of chamber headspace gas was sampled with a gas tight syringe. Samples were analyzed for CO$_2$ on a Shimadzu gas chromatographic-2014 greenhouse gases analyzer. Chamber caps were then removed and 5 mL of water from within was again filtered and analyzed for [DOC]. DOC consumption rate (ΔDOC) was calculated as

$$\Delta DOC = \frac{[DOC]_{initial} - [DOC]_{final}}{incubation \ time \ (d)} \tag{3}$$

[13] DOC mineralization rate (ΔCO$_2$ − C) was calculated as

$$\Delta CO_2 - C = \frac{[CO_2 - C]_{treatment} - [CO_2 - C]_{blank}}{incubation \ time \ (d)} \tag{4}$$

[14] DOC bioavailability was expressed as percent consumed (%bDOC) (ΔDOC divided by [DOC]$_{initial}$) and as percent respired (%bCO$_2$ − C) (ΔCO$_2$ − C divided by [DOC]$_{initial}$).

[15] Areal rate of CO$_2$ release (ΔCO$_2$ − C$_a$, g CO$_2$ − C m^{-2} d^{-1}) was calculated as

$$\Delta CO_2 - C_a = \Delta CO_2 - C \ \times \ V_a \tag{5}$$

where V_a = average areal water volume (L m^{-2}) in the river (equation (2)) and ΔCO$_2$ − C = DOC mineralization rate (g CO$_2$ − C L^{-1} d^{-1}, equation (4)) from chamber incubations.

2.5. DOC Optical Analysis

[16] Emission-excitation matrices (EEMs) were measured for each sample collected in site LR2 from January 2008 to June 2009 (Fluorlog-3; Horiba, Jobin Yvon; University of North Carolina-Chapel Hill) (5 nm slit width), by measuring fluorescence intensity across excitation wavelengths 240–450 nm (5 nm increment) and emission wavelengths 140–950 nm (1 nm increment). All samples were diluted 1:3 with laboratory grade deionized (DI) water, and fluorometer integration times were adjusted between 0.7 and 3.5 s depending on [DOC]. We corrected EEMs for inner filter effects and instrument-specific excitation and emission corrections in MATLAB R2008b (Mathworks) following *Cory et al.* [2010] via a user-generated rhodamine spectrum for excitation correction [*DeRose et al.*, 2007] and a manufacturer-provided emission correction spectrum specific to the CCD detector (Horiba Scientific). We subtracted similarly analyzed blank EEMs, collected from laboratory grade DI water, from sample EEMs. Fluorescence intensities in blank-corrected sample EEMs were converted to Raman units [*Stedmon et al.*, 2003].

[17] From each blank-corrected EEM, fluorescence index (FI), an indicator of terrestrial or aquatic DOC origin, was calculated as the ratio of emission intensity at two wavelengths (470:500 nm), obtained at an excitation wavelength of 370 nm [*McKnight et al.*, 2001], following the protocol in *Cory et al.* [2010]. The FI ranges from approximately 1.2 for terrestrially derived organic matter to approximately 1.5 for autochthonous microbially derived organic matter.

[18] Parallel Factor Analysis (PARAFAC) was conducted to decompose blank-corrected EEMs into unique fluorescence groups representing chemically independent components describing the total EEM [*Stedmon et al.*, 2003]. For each EEM, components are described by F_{max} values. Because the chemical structure of components is unknown, F_{max} values represent maximum fluorescence of each

Table 1. Stepwise Multiple Regression of [DOC] Against Discharge, Temperature, Previous [DOC] (DOC Lag), and Total Discharge During the Previous Hydroperiod, for Each Season[a]

Season	[DOC] (mg L^{-1})	Model R^2_{adj}	Discharge (L d^{-1})	Temperature (°C)	DOC Lag (mg L^{-1})	Previous Hydroperiod Discharge(L)
Fall (22 September to 20 December)	23.41 (0.49)	0.47	$F_{1,34}=9.32$ $p < 0.01$ **0.92 (−)**	*ns*	$F_{1,34}=9.00$ $p < 0.01$ **0.92**	*ns*
Winter (21 December to 19 March)	16.97 (1.52)	0.79	$F_{1,78}=6.48$ $p < 0.05$ **0.89 (−)**	$F_{1,78}=24.40$ $p < 0.0001$ **0.99 (+)**	$F_{1,78}=109.22$ $p < 0.0001$ **0.99**	$F_{1,78}=12.32$ $p < 0.001$ **0.89 (−)**
Spring (20 March to 20 June)	23.59 (3.06)	0.76	$F_{1,52}=13.54$ $p < 0.001$ **0.97 (−)**	$F_{1,52}=6.72$ $p < 0.05$ **0.87 (+)**	$F_{1,52}=8.95$ $p < 0.01$ **0.97**	$F_{1,52}=25.55$ $p < 0.0001$ **0.97 (−)**
Summer (21 June to 21 September)	34.97 (11.96)	0.26	*ns*	*ns*	$F_{1,37}=14.60$ $p < 0.001$ **1.00**	*ns*

[a]Average [DOC] (±1 95% C.I.) and the full model's coefficient of determination (model R^2_{adj}, adjusted for sample size and number of parameters) are provided. Statistical test results are also provided for individual parameters, with each parameter's relative importance weight (from AIC, ranging 0–1) and direction of effect in parentheses. "*ns*" denotes a lack of statistical significance.

component rather than actual concentration. PARAFAC was conducted according to *Stedmon and Bro* [2008] using the DOMFluor toolbox in MATLAB R2008b (Mathworks). Models were validated using split half and random initialization methods [*Stedmon and Bro*, 2008]. Prior to PARAFAC, EEM wavelength ranges were reduced to excitation 250 to 450 nm and emission 320 to 550 nm.

[19] UV visible absorbance was measured on diluted (1:3, as above) samples at 254 nm using a 1 cm path length quartz cuvette on a Perkin Elmer 559 UV/visible spectrophotometer. Specific UV absorbance (SUVA$_{254}$) was calculated by dividing UV absorbance by cuvette path length (meters) and normalizing to [DOC] (mg L^{-1}) [*APHA*, 1999]. SUVA$_{254}$ measures aromatic carbon content of DOC [*Weishaar et al.*, 2003], with smaller SUVA$_{254}$ values (<2 L mg-C^{-1}m^{-1}) associated with lower aromaticity. Average absorbance of diluted samples was 0.23 ± 0.02 absorbance units (AU) (± 1 99% confidence interval [C.I.]), with a maximum absorbance of 0.50 AU. [DOC] was not correlated to Fe, but high Fe concentration (up to 3.08 mg L^{-1}, Table S1) in site LR2 may potentially interfere with SUVA$_{254}$ [*Weishaar et al.*, 2003]. To correct for potential effects of Fe on absorbance (and resulting effects on SUVA$_{254}$), a multiple regression model with DOC and Fe concentration (mg L^{-1}) explaining variability in absorbance ($F_{1,41}=61.98$, $p < 0.0001$, $R^2_{adj}=0.74$) generated a parameter estimate used to correct absorbance according to the following equation:

$$A_{\text{corr}} = A_{254} - \beta_{\text{Fe}} \times [\text{Fe}] \qquad (4)$$

where $A_{\text{corr}}=$ corrected absorbance, $A_{254}=$ absorbance at 254 nm, $\beta_{\text{Fe}}=$ parameter estimate of the effect of Fe (0.07696) on A_{254}, and [Fe]$=$ Fe concentration in mg L^{-1}. *O'Donnell et al.* [2012] used a similar correction factor (0.0687) to adjust absorbance according to Fe in the Yukon River. Our absorbance correction amounted to at most a 0.88 L mg-C^{-1}m^{-1} change in SUVA$_{254}$ for high Fe samples, but a mean correction of 0.39 ± 0.03 (± 1 SE) L mg-C^{-1}m^{-1} for the entire sample set.

2.6. Statistical Analysis

[20] All data sets were analyzed with simple or multiple linear regression (PROC REG at $\alpha = 0.05$) except for changes in %bDOC and %bCO$_2$ − C over time, which were analyzed with analysis of covariance (ANCOVA, PROC GLM at $\alpha = 0.05$) in Statistical Analysis System (SAS) version 9.2 (SAS Institute Inc., Cary, U.S.). Data were log transformed when necessary to meet assumptions of normality, homogeneity of variance, and linearity. When testing for changes in annual dry period length between 1972 and 2009, *t* values were calculated using a heteroskedasticity consistent covariance matrix (PROC REG, option $=$ acov) [*White*, 1980].

[21] To isolate the set of factors best explaining seasonal changes in [DOC] in site L2, the time series was split among seasons delineated by solstices and equinoxes. We used stepwise regression (backward elimination) to identify statistically significant parameters and Akaike's information criterion (AIC) to compare regression models composed of those parameters and to calculate individual parameter importance weights (PROC REG at $\alpha = 0.05$, SAS version 9.2) [*Burnham and Anderson*, 2002]. Explanatory variables were tested for multicollinearity with Pearson's correlation coefficient (*r*) matrices and variance inflation factors. When analyzing the effect of previous hydroperiod discharge or DOC export on current [DOC], the time series was split into hydroperiods. In intermittent rivers (Little River, Okapilco Creek), one hydroperiod ended when river flow ceased for more than 2 weeks. Dry period length was calculated as the number of days without river flow per year. In the Alapaha and Withlacoochee Rivers, which experienced periods of low discharge without cessation of flow, Q70 (daily discharge exceeded 70% of the time period) was calculated from all available USGS data through the year 2000. This was used as an indicator of hydrological drought [*Hisdal et al.*, 2004], which delineated two hydroperiods. One hydroperiod (nondrought conditions) ended when discharge decreased below Q70 for at least 30 days. In all rivers, storm events (isolated continuous flow periods < 60 days) were not analyzed as individual hydroperiods, but their total discharge and DOC export were added to the previous hydroperiod's total. A combination of multiple regression and AIC was also used to analyze the effects of previous hydroperiod discharge and other hydrological variables on [DOC] across rivers within the Suwannee River basin and between decades in site LR2.
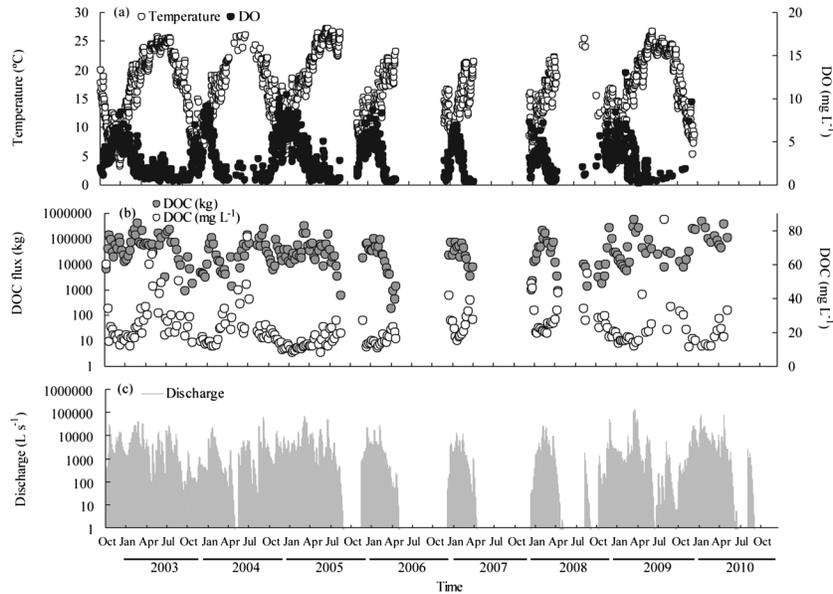
Figure 2. (a) Dissolved oxygen (DO, mg L^{-1}) and temperature (°C), (b) [DOC] (mg L^{-1}, white circles) and DOC export (kg, gray circles), and (c) discharge (L s^{-1}, logarithmic scale) over time from 2002 to 2010 in the Little River (LR2). Average daily temperature, dissolved oxygen, and discharge are provided, while [DOC] is a flow-weighted composite (approximately average). Export was calculated by multiplying [DOC] by water discharged (L) during the sampling period.

3. Results

3.1. [DOC] Drivers

[22] [DOC] was negatively correlated with discharge in site LR2 when analyzed across the time series ($t_{1,232} = -6.998$, $r^2_{adj} = 0.23$, $p < 0.001$, Figure S1), similar to the relationship observed in boreal peatland streams [*Eimers et al.*, 2008].

Total discharge during the previous hydroperiod had a significant negative effect on [DOC] during winter and spring months (Table 1), while average daily discharge in the current hydroperiod had a significant negative relationship with [DOC] during fall, winter, and spring months (Figure 2 and Table 1). [DOC] decreased over time during late fall and early winter, reaching an annual minimum between 8.04 and
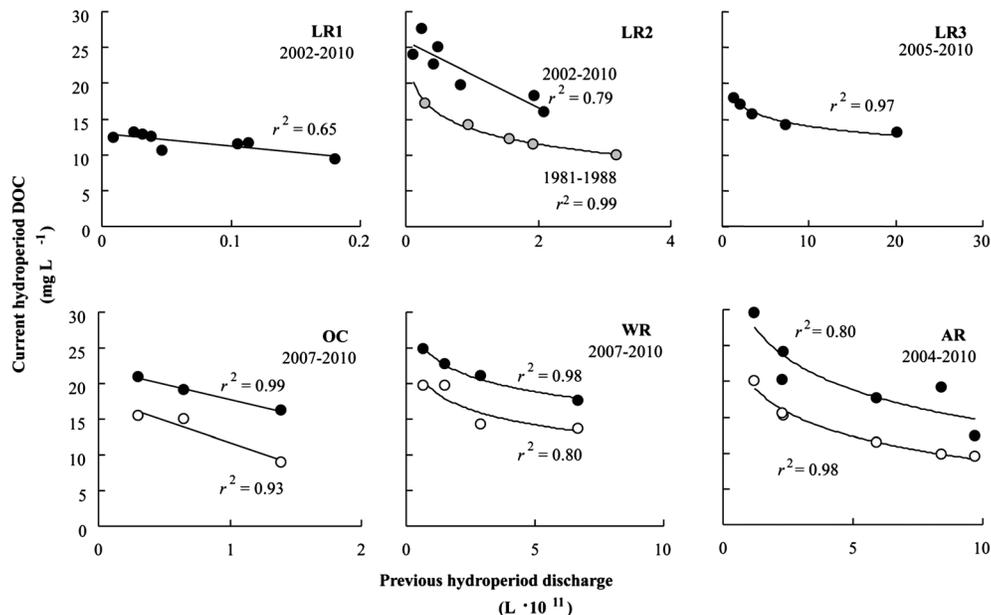
Figure 3. Average (black circles) and minimum (white circles) [DOC] (mg L^{-1}) in the current hydroperiod versus total discharge (L 10^{11}) in the previous hydroperiod for the three Little River sites (LR1–LR3): the Okapilco Creek (OC), the Withlacoochee River (WR), and the Alapaha River (AR). Gray circles in LR2 indicate data collected from 1981 to 1988. Note that *x* axes are in different scales.

Table 2. Comparison of Candidate Multiple Regression Models Explaining Variation in [DOC] Among Hydroperiods and Across Suwannee River Basin Sites LR2, AR, WR, and OC[a]

Suwannee River Basin Sites Candidate Model	K	C_p	R^2_{adj}	AICc	Δ_i	L	w_i
TotalQprev, totalQprev*I	4	2.75	0.76	−83.74	0	1	0.71
TotalQprev, totalQprev*I, medianQ	5	1.51	0.77	−81.94	1.80	0.41	0.29

[a]K is the number of model parameters (including y intercept and slope), C_p is Mallows' C_p, R^2_{adj} is adjusted R^2, AICc is Akaike's information criterion corrected for small sample size, Δ_i is the difference between the candidate and best models' AICc, L is likelihood, and w_i is the relative strength of evidence for each model (between 0 and 1). Parameters initially included were total discharge in the previous hydroperiod (totalQprev), total discharge in the current hydroperiod, current hydroperiod median discharge (medianQ), previous dry period and hydroperiod lengths, average daily discharge during the previous hydroperiod, current hydroperiod length, and the interaction between totalQprev and intermittence (intermittent versus perennial, totalQprev*I).

19.36 mg L^{-1} during early December to mid-February, but rose with increasing temperature in late winter and spring (Figure 2 and Table 1). During summer, [DOC] was higher and more variable than in any other season, peaking between 26.82 and 85.96 mg L^{-1} (Figure 2 and Table 1), but was not significantly correlated with any of the drivers measured in this study. [DOC] was not correlated to chl a, chloride, N, or P concentrations during any season.

3.2. Rainfall, Dry Period Length, and Downstream Exports

[23] In LR2, annual DOC export was negatively correlated to dry period length ($t_{1,7} = 8.71$, $r^2_{adj} = 0.80$, $p < 0.001$), with an annual decrease of approximately 15 t of DOC exported per 1 day increase in annual dry period length. Lower total discharge in one hydroperiod was followed by significantly higher average ($t_{1,5} = -4.37$, $r^2_{adj} = 0.79$, $p < 0.01$) [DOC] in the following hydroperiod (Figure 3). The same negative effect of total hydroperiod discharge on [DOC] in the following hydroperiod was observed in the 1980s (Table 2 and Figure 3), as well as in headwater (LR1) and downstream reaches (LR3) of the LR (Table S2 and Figure 3) and in the Alapaha and Withlacoochee Rivers and Okapilco Creek (Tables 2 and S2 and Figure 3). The magnitude of the effect of total discharge during the previous hydroperiod on [DOC] was larger in truly intermittent, smaller-order river sites (LR2 and OC), as shown by the significant interaction term in Table 2. In site LR2, differences in average temperature had no significant effect on variability in [DOC] among hydroperiods ($t_{1,5} = 0.18$, $r^2 = 0.01$, $p = 0.87$).

[24] The study period (2002–2010) encompassed the range of flow conditions observed since 1972 (Figure 4a), with 2007 being the driest year on record since 1972 in LR2 (no flow for 65% of the year), but with two hydroperiods lasting longer than 1 year (e.g., flow from 31 October 2002 to 25 May 2004). Annual dry period length increased significantly from 1972 to 2010 ($t_{1,37} = 2.33$, $p < 0.05$, $r^2_{adj} = 0.10$, Figure 4a) and became more variable over time (White's test, $x^2_2 = 6.35$, $p = 0.055$), with differences in annual rainfall explaining a significant proportion of the variability ($t_{1,37} = -6.95$, $p < 0.0001$, $r^2_{adj} = 0.56$). However, maximum dry period length per 5 year increment increased dramatically between 1972 and 2010 ($t_{1,6} = 6.34$, $p < 0.001$, $r^2_{adj} = 0.85$, Figure 4b). This was primarily explained by changes in the minimum annual rainfall per 5 year increment ($t_{1,6} = -7.08$, $p < 0.0001$, $r^2_{adj} = 0.88$, Figure 4b), which decreased significantly during the same time period ($t_{1,6} = -14.90$, $p < 0.0001$, $r^2_{adj} = 0.97$, Figure 4b).

3.3. DOC Composition, Mineralization, and Bioavailability

[25] We identified three fluorescent components using the PARAFAC model after removal of outlier EEMs (Figure S2 and Table 3). Comparison of modeled components to PARAFAC models published previously reveals that all three DOC components have characteristics similar to terrestrial humic-like material found in forested streams and wetlands free of wastewater (Table 3). The maximum fluorescence intensities (F_{max}) of these components were positively correlated with each other ($r^2_{adj} \geq 0.95$, $p < 0.0001$) and with [DOC] ($r^2_{adj} \geq 0.74$, $p < 0.0001$) across time, revealing that the overall chemical composition of DOC in the LR was stable throughout changes in [DOC] *preceding* dry periods. However, on the first sample date immediately
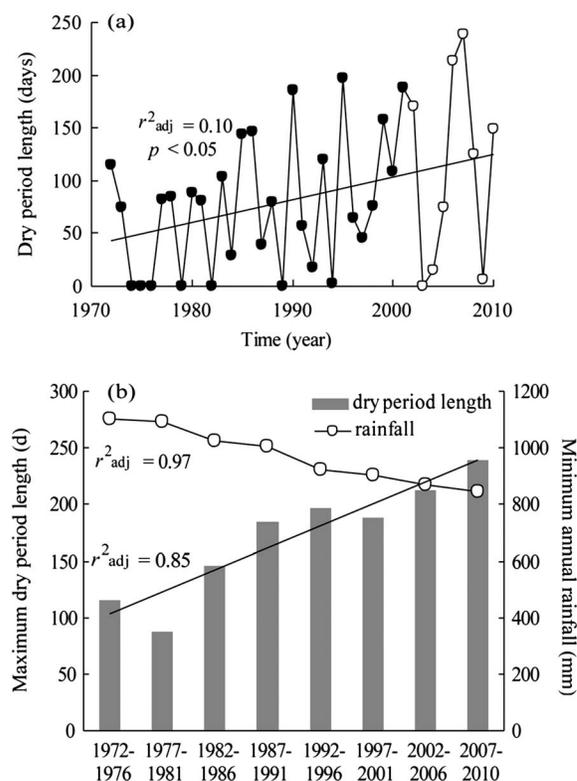
Figure 4. Little River (LR2) (a) annual dry period length over time, with DOC sampling years indicated by open symbols. (b) Maximum annual dry period length (gray columns, days) and minimum annual rainfall (white circles, mm) per 5 year increment from 1972 to 2010.

Table 3. Characterization of Three PARAFAC Components of DOM Identified in This Study, All Resembling Terrestrial Humic-Like Material[a]

Component	Ex. Max. (nm)	Em. Max. (nm)	Description	References
1	<240 (280)	418	Forested streams and wetlands, absent in wastewater	P3(<260,380/498) [*Murphy et al.*, 2008] C3(<250,305/412) [*Stedmon and Markager*, 2005]; C2(<250,305/412) [*Stedmon et al.*, 2003]; A(260/380–460) [*Coble*, 1996]
2	<240 (350)	468	Natural and agricultural catchments, absent in wastewater	C1(<250/448) [*Stedmon and Markager*, 2005] C1(<250/448) [*Stedmon et al.*, 2003]
3	<240 (270) (410)	495	Widespread, high molecular weight	C3(260,370/490), P3(<260,380/498) [*Murphy et al.*, 2008] C3(270,360/478) [*Stedmon et al.*, 2003]

[a]Maximum excitation ("Ex. Max.," secondary excitation peaks in parentheses) and emission wavelengths ("Em. Max.") are provided. Component descriptions are based on similar excitation and emission maxima in the provided references.

following each dry period EEMs were sufficiently different that we had to exclude them as outliers to validate the global PARAFAC model. We assume they include additional uncharacterized chemical components unique to incipient river inundation. Regardless, the fluorescence index (FI) of all samples—including PARAFAC outliers—ranged from 1.32 to 1.48, which is indicative of material of terrestrial detrital origin rather than aquatic microbial origin [*McKnight et al.*, 2001].

[26] DOC mineralization rate ($\Delta CO_2 - C$) was highest at the beginning and end of hydroperiods (Figure 5a), when discharge was low and [DOC] was high. Also positively correlated with [DOC] ($t_{1,43} = 7.19$, $p < 0.0001$, $r^2_{adj} = 0.55$, Figure 5b) and DOC consumption rate (ΔDOC) ($t_{1,43} = 5.36$, $p < 0.0001$, $r^2_{adj} = 0.39$) was $\Delta CO_2 - C$. Similarly, ΔDOC was positively correlated with [DOC] ($t_{1,43} = 7.52$, $p < 0.0001$, $r^2_{adj} = 0.57$, Figure 5b). Estimated CO_2 release per m^2 was less variable over

time but was highest at high flows, averaging 0.22 ± 0.03 (± 1 SE) and ranging 0.07–1.05 g $CO_2 - C$ m^{-2} (Figure 5a).

[27] Average DOC bioavailability expressed as % consumed (%bDOC = 19.39 ± 1.14 [± 1 SE]) and % respired (% $bCO_2 - C = 14.39 \pm 0.97$ [± 1 SE], Figure 6a) were similar, ranging from -2 to 37% of initial DOC. There was no significant difference in %bDOC between years ($F_{1,19} = 0.43$, $p = 0.52$) or among months ($F_{1,19} = 3.01$, $p = 0.099$) in 2008 and 2009. However, %bCO_2 did differ among months ($F_{1,19} = 4.45$, $p < 0.05$, Figure 6a). Uncorrected SUVA_{254}, an indicator of percent aromaticity (high values indicate higher relative abundance of aromatic rings), was negatively correlated with ΔDOC (mg L^{-1} d^{-1}) ($t_{1,42} = -6.15$, $p < 0.0001$, $r^2_{adj} = 0.46$), and $\Delta CO_2 - C$ (mg L^{-1} d^{-1}) ($t_{1,42} = -5.95$, $p < 0.0001$, $r^2_{adj} = 0.45$, Figure 6b). The dry-wet transition period samples (Figure 6b, indicated with triangles) had among
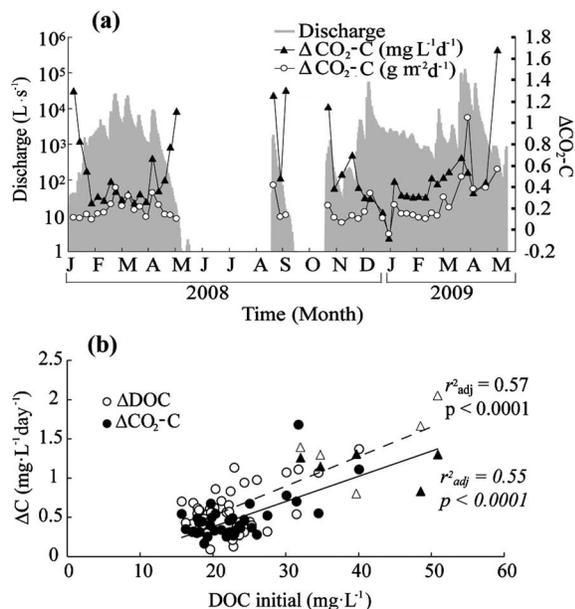
Figure 5. Little River (LR2) (a) DOC mineralization rate (mg $CO_2 - C$ L^{-1} d^{-1}, black triangles and g $CO_2 - C$ m^2 d^{-1}, white circles) and discharge (L s^{-1}, logarithmic scale). (b) Dashed line is ΔDOC (white symbols) and solid line is $\Delta CO_2 - C$ (black symbols) (mg C L^{-1} d^{-1}) regressed against [DOC] (mg L^{-1}).
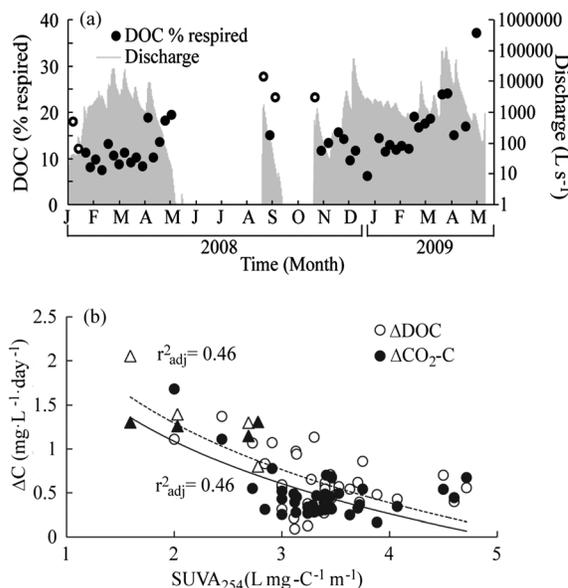
Figure 6. Little River (LR2) (a) DOC bioavailability (% $bCO_2 - C$) over time in 2008 and 2009, with discharge (L · s^{-1}, logarithmic scale). Black symbols with white central points indicate outliers not included in PARAFAC models. (b) Dashed line is ΔDOC (white symbols) and solid line is $\Delta CO_2 - C$ (black symbols) (mg C L^{-1} d^{-1}) regressed against uncorrected SUVA_{254}. Outliers, collected during wet-dry transition periods, are indicated with triangles.

the lowest $SUVA_{254}$ values of all samples, consistent with fluorescence analysis that suggested unique chemical properties of these samples. Correcting $SUVA_{254}$ values for Fe did not substantially alter this relationship or the correlation with DOC consumption (ΔDOC $t_{1,42} = -5.41$, $p < 0.0001$, $r^2_{adj} = 0.40$) or mineralization rates ($\Delta CO_2 - C$ $t_{1,42} = -6.38$, $p < 0.0001$, $r^2_{adj} = 0.48$).

4. Discussion

[28] Our results suggest DOC concentrations and carbon mineralization rates are coupled to DOC export during the prior season's hydroperiod. Short seasonal hydroperiods, resulting from extended drought, export less DOC than longer hydroperiods but also appear to prime the riverine system for high [DOC] in the following season (Figure 3). Organic matter accumulates during dry years as a result of slow decomposition, and in addition to fresh leaf litter inputs [*Mehring*, 2012], leads to a large pool of accumulated soluble carbon and consequently higher [DOC] during the following wet period (Figure 3). This may in turn stimulate higher DOC mineralization rates, supported by the strong positive correlation we observed between DOC mineralization rate and [DOC] in our laboratory incubations (Figure 5b). If these climate trends continue, the net effect may be a more localized riverine carbon cycling with lower downstream transport of DOC but higher local mineralization rates.

[29] While mineralization rates may be enhanced during drier years in the LR, it is not clear if this will result in greater gaseous carbon export throughout the stream network. Despite higher mineralization rates at low discharge, we estimate total areal release of CO_2 ($\Delta CO2 - C$ [g m^{-2} d^{-1}], Figure 5a) to be slightly elevated at higher discharge because of greater water volume and thus a greater amount of DOC per m^2 under those conditions. Accordingly, as rainfall and discharge decrease, the system may retain more carbon due to decreased dissolved transport as well as decreased CO_2 emissions. Extended dry periods and reduced discharge resulted in substantial reductions in DOC export, and were followed by elevated [DOC] at three monitoring sites within the LR, and in three other large blackwater rivers of the Suwannee River basin (Figure 3). However, to fully understand the effects on CO_2 release, the relationship between DOC concentration and mineralization must be quantified in additional sites throughout the Suwannee River basin, and relative fluxes of CO_2 during dry periods should also be assessed.

[30] The possibility exists for some dependence of current discharge rates on total discharge or dry period length preceding the current hydroperiod. The hyporheic zone provides considerable water storage capacity and creates a surficial aquifer in the Little River [*Shirmohammadi et al.*, 1986]. Therefore, stream flow may be lower following droughts due to the vast capacity for storage within the highly extensive stream network. The lower flow during the initial period of rewetting may result in higher [DOC], in addition to the turnover of organic matter that accumulated during the dry period. However, the effects of total discharge or DOC export in the previous hydroperiod are detectable far into the current hydroperiod (throughout winter and spring, Table 1) and neither previous hydroperiod discharge nor previous dry period length was significantly correlated to average or median discharge during the current hydroperiod or during the first 30 days of the current hydroperiod. While median daily discharge does explain some variability in average [DOC], previous hydroperiod discharge was by far the best predictor of [DOC] among hydroperiods (Tables 2 and S2 and Figure 3). Therefore, although the two may be related, we suggest antecedent flow conditions impact [DOC] separately from current flow conditions.

[31] Optical analyses reveal unique DOC characteristics during the wet-dry transition phases consistent with a high bioavailablity. Wet-dry transition DOC had among the lowest SUVA values we recorded and substantially different fluorescence emission values than our other samples. These chemical characteristics are consistent with a highly labile dissolved organic matter (DOM) pool with a low density of aromatic moieties. Laboratory incubations of this DOC consistently had elevated bioavailability (%bCO_2, Figure 6a) and mineralization rates (Figure 5a), suggesting rapid carbon cycling during these transition periods.

[32] We identified three potential drivers of [DOC] in the LR: temperature, discharge, and antecedent hydrological conditions. The importance of each one varied seasonally (Table 1), but each is likely to increase in intensity with climate change. The initially high [DOC] observed during late fall and early winter, when flow usually resumed in the LR, may have been due to a large pulse of DOC from soil pore water and accumulated leaf litter [*Meyer et al.*, 1998; *Vázquez et al.*, 2007]. [DOC] subsequently decreased as discharge increased (Figures 2 and 3), possibly due to a dilution effect. There is considerable model uncertainty regarding long-term changes in rainfall patterns through the southeastern U.S. [*Solomon et al.*, 2009]. Even in the event of no change or moderate increases in rainfall, evapotranspiration is predicted to exceed precipitation, and thus, reductions in river discharge throughout middle and low latitudes are expected [*Dai*, 2010; *Mulholland et al.*, 1997; *Nijssen et al.*, 2001]. Reduced river discharge may make elevated [DOC] a more common occurrence. As winter and spring progressed in our study, [DOC] was positively correlated with rising temperatures (Table 1 and Figure 2), possibly due to enhanced microbial activity and DOC release. Water temperatures may further enhance DOC release if they continue to rise through further climatic warming [*Kaushal et al.*, 2010].

[33] The negative effects of decreased river flow on DOC flux are likely to be exacerbated by increasing human water demand [*Vörösmarty et al.*, 2000]. For example, the southeastern U.S. has experienced dramatic widespread increases in farm pond construction [*De Steven and Lowrance*, 2011] and center pivot irrigation [*Mullen et al.*, 2009] over the past few decades. While farm ponds are not likely to have an impact during periods of adequate rainfall, impoundment of water and withdrawal for irrigation during the growing season likely contribute to low flows [*Lowrance et al.*, 2007], thereby lengthening dry periods and indirectly affecting carbon cycling.

[34] Riverine transport makes up the largest input of terrigenous DOC to oceans [*Meybeck*, 1982], and riverine microbial processing of DOC releases substantial amounts of greenhouse gas to the atmosphere [*Cole et al.*, 2007]. Climatic changes including global alterations to temperature and river discharge may substantially alter both of these

major global carbon cycling pathways. Our results illustrate strong effects of local climatic conditions on carbon cycling in southeastern blackwater rivers, whereby decreased annual rainfall and river discharge lead to decreased riverine DOC export to downstream reaches but elevated DOC concentrations that potentially enhance local mineralization rates. These carbon cycle alterations may perturb ecosystem function at regional scales, affecting CO_2 emissions throughout large river systems, as well as DOC delivery from terrestrial to marine ecosystems.

References

Alexandrov, V. A., and G. Hoogenboom (2001), Climate variation and crop production in Georgia, USA, during the twentieth century, *Clim. Res.*, *17*, 33–43.

American Public Health Association (1999), *Standard Methods for the Examination of Water and Wastewater*, 1325 pp., American Public Health Association Publication, APHA, AWWA, WEF, Washington, D. C.

Baum, A., T. Rixen, and J. Samiaji (2007), Relevance of peat draining rivers in central Sumatra for the riverine input of dissolved organic carbon into the ocean, *Estuarine Coastal Shelf Sci.*, *73*(3-4), 563–570, doi:10.1016/j.ecss.2007.02.012.

Beck, K. C., J. H. Reuter, and E. M. Perdue (1974), Organic and inorganic geochemistry of some coastal plain rivers of the southeastern United States, *Geochim. Cosmochim. Acta*, *38*(3), 341–364, doi:10.1016/0016-7037(74)90130-6.

Berggren, M., L. Ström, H. Laudon, J. Karlsson, A. Jonsson, R. Giesler, A. K. Bergström, and M. Jansson (2010), Lake secondary production fueled by rapid transfer of low molecular weight organic carbon from terrestrial sources to aquatic consumers, *Ecol. Lett.*, *13*(7), 870–880, doi:10.1111/j.1461-0248.2010.01483.x.

Bianchi, T. S. (2011), The role of terrestrially derived organic carbon in the coastal ocean: A changing paradigm and the priming effect, *Proc. Natl. Acad. Sci. U. S. A.*, *108*(49), 19,473–19,481, doi:10.1073/pnas.1017982108.

Bledsoe, E. L., and E. J. Phlips (2000), Relationships between phytoplankton standing crop and physical, chemical, and biological gradients in the Suwannee River and plume region, U.S.A, *Estuaries*, *23*(4), 458–473.

Bosch, D. D., and J. M. Sheridan (2007), Stream discharge database, Little River Experimental Watershed, Georgia, United States, *Water Resour. Res.*, *43*, W09473, doi:10.1029/2006WR005833.

Bosch, D. D., J. M. Sheridan, R. R. Lowrance, R. K. Hubbard, T. C. Strickland, G. W. Feyereisen, and D. G. Sullivan (2007), Little River Experimental Watershed database, *Water Resour. Res.*, *43*, W09470, doi:10.1029/2006WR005844.

Burnham, K. P., and D. R. Anderson (2002), *Model Selection and Multimodel Inference: A Practical Information-Theoretic Approach*, 488 pp., Springer, New York.

Chow, A. T., K. K. Tanji, S. Gao, and R. A. Dahlgren (2006), Temperature, water content and wet-dry cycle effects on DOC production and carbon mineralization in agricultural peat soils, *Soil Biol. Biochem.*, *38*(3), 477–488, doi:10.1016/j.soilbio.2005.06.005.

Coble, P. G. (1996), Characterization of marine and terrestrial DOM in seawater using excitation-emission matrix spectroscopy, *Mar. Chem.*, *51*(4), 325–346, doi:10.1016/0304-4203(95)00062-3.

Cole, J. J., et al. (2007), Plumbing the global carbon cycle: Integrating inland waters into the terrestrial carbon budget, *Ecosystems*, *10*(1), 172–184, doi:10.1007/s10021-006-9013-8.

Cory, R. M., M. P. Miller, D. M. McKnight, J. J. Guerard, and P. L. Miller (2010), Effect of instrument-specific response on the analysis of fulvic acid fluorescence spectra, *Limnol. Oceanogr. Methods*, *8*, 67–78, doi:10.4319/lom.2010.8.67.

Dai, A. (2010), Drought under global warming: A review, *WIREs Clim. Change*, *2*(1), 45–65, doi:10.1002/wcc.81.

Dai, A., T. Qian, K. E. Trenberth, and J. D. Milliman (2009), Changes in continental freshwater discharge from 1948 to 2004, *J. Clim.*, *22*(10), 2773–2792.

De Steven, D., and R. Lowrance (2011), Agricultural conservation practices and wetland ecosystem services in the wetland-rich Piedmont-Coastal Plain region, *Ecol. Appl.*, *21*(3), S3–S17.

DeRose, P. C., E. A. Early, and G. W. Kramer (2007), Qualification of a fluorescence spectrometer for measuring true fluorescence spectra, *Rev. Sci. Instrum.*, *78*(3), 033,107, doi:10.1063/1.2715952.

Eimers, M. C., J. Buttle, and S. A. Watmough (2008), Influence of seasonal changes in runoff and extreme events on dissolved organic carbon trends in wetland- and upland-draining streams, *Can. J. Fish. Aquat. Sci.*, *65*(5), 796–808, doi:10.1139/f07-194.

Feyereisen, G. W., R. Lowrance, T. C. Strickland, J. M. Sheridan, R. K. Hubbard, and D. D. Bosch (2007), Long-term water chemistry database, Little River Experimental Watershed, southeast Coastal Plain, United States, *Water Resour. Res.*, *43*, W09474, doi:10.1029/2006WR005835.

Findlay, S. E. G. (2005), Increased carbon transport in the Hudson River: Unexpected consequence of nitrogen deposition?, *Front. Ecol. Environ.*, *3*(3), 133–137.

Findlay, S. E. G., R. L. Sinsabaugh, W. V. Sobczak, and M. Hoostal (2003), Metabolic and structural response of hyporheic microbial communities to variations in supply of dissolved organic matter, *Limnol. Oceanogr.*, *48*(4), 1608–1617, doi:10.4319/lo.2003.48.4.1608.

Freeman, C., C. D. Evans, D. T. Monteith, B. Reynolds, and N. Fenner (2001), Export of organic carbon from peat soils, *Nature*, *412*(6849), 785, doi:10.1038/35090628.

Freeman, C., N. Fenner, N. J. Ostle, H. Kang, D. J. Dowrick, B. Reynolds, M. A. Lock, D. Sleep, S. Hughes, and J. Hudson (2004), Export of dissolved organic carbon from peatlands under elevated carbon dioxide levels, *Nature*, *430*(6996), 195–198, doi:10.1038/nature02707.

Hanson, P. C., D. L. Bade, S. R. Carpenter, and T. K. Kratz (2003), Lake metabolism: Relationships with dissolved organic carbon and phosphorus, *Limnol. Oceanogr.*, *48*(3), 1112–1119.

Hisdal, H., L. Tallaksen, B. Clausen, E. Peters, and A. Gustard (2004), Hydrological drought characteristics, in *Hydrological Drought: Processes and Estimation Methods for Streamflow and Groundwater*, edited by L. Tallaksen and H. Van Lanen, pp. 139–182, Elsevier, Amsterdam.

Kankaala, P., and I. Bergström (2004), Emission and oxidation of methane in Equisetum fluviatile stands growing on organic sediment and sand bottoms, *Biogeochemistry*, *67*(1), 21–37.

Kaushal, S. S., G. E. Likens, N. A. Jaworski, M. L. Pace, A. M. Sides, D. Seekell, K. T. Belt, D. H. Secor, and R. L. Wingate (2010), Rising stream and river temperatures in the United States, *Front. Ecol. Environ.*, *8*(9), 461–466, doi:10.1890/090037.

Larsen, S., T. Andersen, and D. O. Hessen (2011), Climate change predicted to cause severe increase of organic carbon in lakes, *Global Change Biol.*, *17*(2), 1186–1192, doi:10.1111/j.1365-2486.2010.02257.x.

Leopold, L. B., and T. Maddock (1953), *The Hydraulic Geometry of Stream Channels and Some Physiographic Implications*, U.S. Geological Survey Professional paper No. 252, US Government Printing Office, Washington, D. C.

Lowrance, R., J. M. Sheridan, R. G. Williams, D. D. Bosch, D. G. Sullivan, D. R. Blanchett, L. M. Hargett, and C. M. Clegg (2007), Water quality and hydrology in farm-scale coastal plain watersheds: Effects of agriculture, impoundments, and riparian zones, *J. Soil Water Conserv.*, *62*(2), 65–76.

Lundquist, E. J., L. E. Jackson, and K. M. Scow (1999), Wet-dry cycles affect dissolved organic carbon in two California agricultural soils, *Soil Biol. Biochem.*, *31*(7), 1031–1038.

Lutz, B. D., P. J. Mulholland, and E. S. Bernhardt (2012), Long-term data reveal patterns and controls on streamwater chemistry in a forested stream: Walker Branch, Tennessee, *Ecol. Monogr.*, *82*, 367–387, doi:10.1890/11-1129.1.

McDowell, W. H., A. Zsolnay, J. A. Aitkenhead-Peterson, E. G. Gregorich, D. L. Jones, D. Jödemann, K. Kalbitz, B. Marschner, and D. Schwesig (2006), A comparison of methods to determine the biodegradable dissolved organic carbon from different terrestrial sources, *Soil Biol. Biochem.*, *38*(7), 1933–1942, doi:10.1016/j.soilbio.2005.12.018.

McKnight, D. M., E. W. Boyer, P. K. Westerhoff, P. T. Doran, T. Kulbe, and D. T. Andersen (2001), Spectrofluorometric characterization of dissolved organic matter for indication of precursor organic material and aromaticity, *Limnol. Oceanogr.*, *46*(1), 38–48, doi:10.4319/lo.2001.46.1.0038.

Mehring, A. S. (2012), Effects of organic matter processing on oxygen demand in a south Georgia blackwater river, dissertation thesis, 211 pp., The University of Georgia, Athens, Ga.

Meybeck, M. (1982), Carbon, nitrogen, and phosphorus transport by world rivers, *Am. J. Sci.*, *282*(4), 401–450.

Meyer, J. L. (1992), Seasonal patterns of water quality in blackwater rivers of the Coastal Plain, southeastern United States, in *Water Quality in North American River Systems*, edited by C. D. Becker and D. A. Neitzel, pp. 250–276, Battelle Press, Columbus.

Meyer, J. L., J. B. Wallace, and S. L. Eggert (1998), Leaf litter as a source of dissolved organic carbon in streams, *Ecosystems*, *1*(3), 240–249.

Monteith, D. T., et al. (2007), Dissolved organic carbon trends resulting from changes in atmospheric deposition chemistry, *Nature*, *450*(7169), 537–540.

Mulholland, P. J., and E. J. Kuenzler (1979), Organic carbon export from upland and forested wetland watersheds, *Limnol. Oceanogr.*, *24*(5), 960–966.

Mulholland, P. J., G. R. Best, C. C. Coutant, G. M. Hornberger, J. L. Meyer, P. J. Robinson, J. R. Stenberg, R. E. Turner, F. Vera-Herrera, and R. G. Wetzel (1997), Effects of climate change on freshwater ecosystems of the south-eastern United States and the Gulf Coast of Mexico, *Hydrol. Processes*, *11*(8), 949–970, doi:10.1002/(sici)1099-1085(19970630)11:8<949::aid-hyp513>3.3.co;2-7.

Mullen, J. D., Y. Yu, and G. Hoogenboom (2009), Estimating the demand for irrigation water in a humid climate: A case study from the southeastern United States, *Agric. Water Manage.*, *96*(10), 1421–1428, doi:10.1016/j.agwat.2009.04.003.

Murphy, K. R., C. A. Stedmon, T. D. Waite, and G. M. Ruiz (2008), Distinguishing between terrestrial and autochthonous organic matter sources in marine environments using fluorescence spectroscopy, *Mar. Chem.*, *108*(1-2), 40–58, doi:10.1016/j.marchem.2007.10.003.

Nijssen, B., G. M. O'Donnell, A. F. Hamlet, and D. P. Lettenmaier (2001), Hydrologic sensitivity of global rivers to climate change, *Clim. Change*, *50*(1), 143–175.

O'Donnell, J. A., G. R. Aiken, M. A. Walvoord, and K. D. Butler (2012), Dissolved organic matter composition of winter flow in the Yukon River basin: Implications of permafrost thaw and increased groundwater discharge, *Global Biogeochem. Cycles*, *26*, GB0E06, doi:10.1029/2012GB004341.

Pärn, J., and Ü. Mander (2012), Increased organic carbon concentrations in Estonian rivers in the period 1992–2007 as affected by deepening droughts, *Biogeochemistry*, *108*(1-3), 351–358, doi:10.1007/s10533-011-9604-0.

Pederson, N., et al. (2012), A long-term perspective on a modern drought in the American Southeast, *Environ. Res. Lett.*, *7*(1), 014,034, doi:10.1088/1748-9326/7/1/014034.

Pulliam, W. M. (1993), Carbon dioxide and methane exports from a southeastern floodplain swamp, *Ecol. Monogr.*, *63*(1), 29–53.

Raymond, P. A., and J. E. Bauer (2001), Riverine export of aged terrestrial organic matter to the North Atlantic Ocean, *Nature*, *409*(6819), 497–500, doi:10.1038/35054034.

Rixen, T., A. Baum, T. Pohlmann, W. Balzer, J. Samiaji, and C. Jose (2008), The Siak, a tropical black water river in central Sumatra on the verge of anoxia, *Biogeochemistry*, *90*(2), 129–140, doi:10.1007/s10533-008-9239-y.

Schlesinger, W. H., and J. M. Melack (1981), Transport of organic carbon in the world's rivers, *Tellus*, *33*(2), 172–187, doi:10.1111/j.2153-3490.1981.tb01742.x.

Seager, R., A. Tzanova, and J. Nakamura (2009), Drought in the southeastern United States: Causes, variability over the last millennium, and the potential for future hydroclimate change, *J. Clim.*, *22*(19), 5021–5045.

Sheridan, J. M. (1997), Rainfall-streamflow relations for coastal plain watersheds, *Appl. Eng. Agric.*, *13*(3), 333–344.

Shirmohammadi, A., J. M. Sheridan, and L. E. Asmussen (1986), Hydrology of alluvial stream channels in southern Coastal Plain watersheds, *Trans. ASAE*, *29*(1), 135–142.

Solomon, S., G.-K. Plattner, R. Knutti, and P. Friedlingstein (2009), Irreversible climate change due to carbon dioxide emissions, *Proc. Natl. Acad. Sci. U. S. A.*, *106*(6), 1704–1709, doi:10.1073/pnas.0812721106.

Stahle, D. W., and M. K. Cleaveland (1992), Reconstruction and analysis of spring rainfall over the southeastern US for the past 1000 years, *Bull. Am. Meteorol. Soc.*, *73*(12), 1947–1961.

Stedmon, C. A., and R. Bro (2008), Characterizing dissolved organic matter fluorescence with parallel factor analysis: A tutorial, *Limnol. Oceanogr. Methods*, *6*, 572–579.

Stedmon, C. A., and S. Markager (2005), Resolving the variability of dissolved organic matter fluorescence in a temperate estuary and its catchment using PARAFAC analysis, *Limnol. Oceanogr.*, *50*(2), 686–697, doi:10.4319/lo.2005.50.2.0686.

Stedmon, C. A., S. Markager, and R. Bro (2003), Tracing dissolved organic matter in aquatic environments using a new approach to fluorescence spectroscopy, *Mar. Chem.*, *82*(3–4), 239–254, doi:10.1016/s0304-4203(03)00072-0.

United States Environmental Protection Agency (1998), *Method 445.0 In Vitro Determination of Chlorophyll a and Pheophytin a in Marine and Freshwater Algae by Fluorescence*, Revision 1.2, National Exposure Research Laboratory, Office of Research and Development, Cincinnati, Ohio.

Vázquez, E., A. M. Romaní, F. Sabater, and A. Butturini (2007), Effects of the dry-wet hydrological shift on dissolved organic carbon dynamics and fate across stream-riparian interface in a Mediterranean catchment, *Ecosystems*, *10*(2), 239–251, doi:10.1007/s10021-007-9016-0.

Vörösmarty, C. J., P. Green, J. Salisbury, and R. B. Lammers (2000), Global water resources: Vulnerability from climate change and population growth, *Science*, *289*(5477), 284–288, doi:10.1126/science.289.5477.284.

Weishaar, J. L., G. R. Aiken, B. A. Bergamaschi, M. S. Fram, R. Fujii, and K. Mopper (2003), Evaluation of specific ultraviolet absorbance as an indicator of the chemical composition and reactivity of dissolved organic carbon, *Environ. Sci. Technol.*, *37*(20), 4702–4708.

White, H. (1980), A heteroskedasticity-consistent covariance matrix estimator and a direct test for heteroskedasticity, *Econometrica*, *48*(4), 817–838.

Wiegner, T. N., L. A. Kaplan, J. D. Newbold, and P. H. Ostrom (2005), Contribution of dissolved organic C to stream metabolism: A mesocosm study using 13 C-enriched tree-tissue leachate, *J. North Am. Benthological Soc.*, *24*(1), 48–67, doi:10.1899/0887-3593(2005)024<0048:codoct>2.0.co;2.